



# Correction of the probabilistic density function of discontinuities spacing considering the statistical error based on negative exponential distribution

Jianhong Ye<sup>a,b,d,\*</sup>, Yan Zhang<sup>c</sup>, Jinzhong Sun<sup>b</sup>, Faquan Wu<sup>a</sup>

<sup>a</sup> Key Laboratory of Engineering Geomechanics, Institute of Geology and Geophysics, Chinese Academy of Sciences, Beijing 100029, China

<sup>b</sup> Department of Civil Engineering, School of Engineering and Technology, China University of Geosciences, Beijing 100083, China

<sup>c</sup> Department of Civil and Environmental Engineering, University of Science and Technology Beijing, Beijing 100083, China

<sup>d</sup> Division of Civil Engineering, University of Dundee, Dundee DD1 4HN, UK

## ARTICLE INFO

### Article history:

Received 24 January 2012

Received in revised form

21 March 2012

Accepted 16 April 2012

Available online 25 April 2012

### Keywords:

Probabilistic density function

Spacing of discontinuities

Statistical error

Negative exponential distribution

Monte Carlo

Fractured rock mass

## ABSTRACT

The mechanical and hydraulic properties of fractured rock masses are generally controlled by the distribution characteristics of discontinuities developed in the rock masses. In practical measurement on exposures, the spacing data collected frequently contains some statistical errors due to the spacing of small discontinuities, and micro-cracks being ignored. In this study, a correction model aiming to eliminate the statistical error is proposed based on the negative exponential distribution of trace length and spacing, to describe the distribution regularity of the spacing data obtained from outcrops or exposures. Based on the model, a corrected probabilistic density function that can describe the distribution regularity of the spacing data containing the statistical error is developed; and a new method is further presented to determine the true distribution parameter of spacing of all discontinuities in rock masses. The sensitivity analysis indicates that the true distribution parameter  $\lambda$  of all spacing is moderately sensitive to the  $\mu$  (reciprocal of the mean trace length) and the critical trace length  $l_0$ ; and completely insensitive to the maximum spacing of small discontinuities  $x_0$ . Finally, the correction theory is verified by a simple 2D model with one set of discontinuities and a complex 2D model with four sets of discontinuities, generated using Monte Carlo method.

© 2012 Elsevier Ltd. All rights reserved.

## 1. Introduction

Discontinuities developed in rock masses, such as fractures and joints, have significant influences on the deformation (Lin et al., 1996), strength (Kulatilake et al., 1997), permeability (Larsen et al., 2009; Baghbanan and Jing, 2007), stress–strain relation (Tai and Huang, 2009), and the failure (Liu et al., 2000) of rock masses. Generally, the discontinuities are developed in rock masses randomly and in sets. The properties of the fracture networks in rock masses, including the trace, spacing and orientation play the dominant role in the instability of rock-slopes, landfall of rock blocks and the failure of surrounding rock of caverns. The development characteristics of discontinuities are always paid great attention in the large-scale construction engineering, such as the Three Gorge dam (Kulatilake et al., 1996), Jinping NO.1 and 2 hydropower stations (Deng et al., 1996) in China.

The trace length and spacing are two parameters usually used to describe the geometrical characteristics of the fracture network of

discontinuities. They are both considered to be generated in rock masses randomly; and could be frequently described by certain probabilistic density functions. Priest and Hudson (1976, 1981) and Einstein and Beacher, 1983 had conducted the path-breaking works on this problem, and reported that the statistical regularity of trace length and spacing of discontinuities both complied with the negative exponential distributions. Many field measurements also shown that the negative exponential probabilistic density distribution is suitable to represent the distribution regularity of trace length (Wallis and King, 1980; Baecher, 1983; Kulatilake et al., 1993, 2003; Park and West, 2001), and the spacing of discontinuities (Gillespie et al., 1993; Narr and Suppe, 1991; Zhou et al., 2000; Zhang et al., 2007).

However, there is also some literature claiming that the spacing of discontinuities in rock masses follow well the lognormal distribution. Castaing et al. (1997) studied the scale effect of natural fracture networks on geological maps of different scales. It is found that the spacing of fractures can be described by the lognormal law at some scale, such as 1:1, 1:100 and 1:1000. Pascal and Angelier (1997) have collected the field data from some coastal exposures in Liassic rocks at Liantwit Major near Cardiff (Wales, U. K.). It is found that the data of spacing of discontinuities in rock masses fits

\* Corresponding author. University of Dundee, Division of Civil Engineering, Dundee DD1 4HN, UK.

E-mail address: [yejianhongcas@gmail.com](mailto:yejianhongcas@gmail.com) (J. Ye).

well the lognormal distribution. The data of discontinuity spacing measured by Ruf et al. (1998), and Sari (2009) from outcrops both show a good consistency with the lognormal distribution. Simpson (2000) concluded that spacing was neither well described by the power law, nor by the negative exponential distribution, but fitted the lognormal distribution based on the data collected from veins in Psammite and Pelite, NW Sardinia Italy. Odonne et al. (2007) found that the spacing of discontinuities not only in each sedimentary layer, but also in the whole statistical window, both complied well with the lognormal distribution.

It is well known that there are not only large and visible discontinuities, but also a great number of small, and invisible discontinuities in fractured rock masses. The number of small and invisible discontinuities is large, and the spacing between them is small. Correspondingly, the frequency of spacing near zero is high, and decreases when the value of spacing increases. In mathematics, the negative exponential distribution can be used to describe this kind of distribution regularity. Therefore, the spacing of all discontinuities in fractured rock masses is frequently described by the negative exponential distribution in practical engineering (Priest and Hudson, 1976, 1981; Einstein and Beacher, 1983). Further research by Lemy and Hadjigeorgiou (2003) and Zhang and Einstein (1998) indicated that whether the spacing of discontinuities follows the negative exponential law or the lognormal law is mainly dependent on the minimum measurement size (MMS), namely the minimum length of discontinuities which are measured by operators on exposures. If the MMS is small, for example, 10 mm, the spacing obtained fits well the negative exponential distribution (Priest and Hudson, 1976, 1981). If the MMS is large, for example 50 cm, a great number of small discontinuities will be ignored in the field measurement. The spacing of discontinuities obtained from field outcrops will follow the lognormal law. Actually, the two types of distribution would both be accurate. The only difference between them is that there is much more statistical error contained in the spacing data if the large MMS is adopted due to the fact that a great number of small discontinuities are ignored during field measurement.

In practical measurement, the method adopting the statistical window or scan-line is widely used to measure the trace length and the spacing of discontinuities on field outcrops, rock cuts or tunnel walls. However, no matter which method is adopted, the measurement scope is always finite. Therefore, the maximum spacing obtained is limited. Additionally, the small discontinuities are frequently ignored due to the fact that they are either hidden in the rock masses, or are difficult to check in the process of measuring at worksites. Some statistical errors are unavoidable in the data of spacing and trace length obtained from worksites. Some literature (Toth, 2009; Priest, 2004; Lemy and Hadjigeorgiou, 2003; Warburton, 1980; Zhang and Einstein, 1998; Mauldon, 1998) has also found this kind of statistical error. For the trace length, some correction methods aiming to eliminate the statistical error have been developed (Zhang and Einstein, 1998; Mauldon, 1998; Priest, 2004; Warburton, 1980) when estimating the mean trace or performing the mechanical or hydraulic computation. For spacing data collected from field exposures, the statistical error also exists. However, little attention has been paid to it; and few studies have been conducted to correct this kind of statistical error. In order to accurately estimate the characteristics of deformation, strength and permeability of fractured rock masses with the spacing data obtained from worksites or outcrops, it is meaningful to develop a correction model to eliminate the statistical error of spacing.

In this study, a new correction method, aiming to eliminate the statistical error of spacing data collected from worksites or outcrops is proposed based on the negative exponential distribution. Adopting the proposed method, a corrected probabilistic density function  $f_2(x)$  which can describe the distribution regularity of the

spacing data obtained from worksites or outcrops is derived. Based on the corrected probabilistic density function  $f_2(x)$ , a formula is developed to determine the true distribution parameter of spacing of all discontinuities using the spacing data collected from worksites or outcrops; Finally, a simple 2D model with only one set of discontinuities, and a complex 2D model with four sets of discontinuities are generated adopting the Monte Carlo method, and are used to check the validity of the corrected model and the formulas.

## 2. Development of correction theory

Based on the results reported in previous literature, it is assumed that the trace length and spacing of discontinuities in fractured rock masses both naturally follow the negative exponential distribution on the whole. In rock engineering, the negative exponential distribution is widely adopted to estimate the Rock Quality Designation (RQD) adopting the estimation formula proposed by Priest and Hudson (1981):

$$RQD = 100e^{-0.1\lambda}(0.1\lambda + 1)$$

in which  $\lambda$  is the distribution parameter of the negative exponential distribution of spacing. In practical rock engineering, the RQD is a very important parameter used to determine the rock quality, to classify the rock classification, and to assess the stability of slopes, tunnels or excavated caverns in mountains. From the point of practicality in engineering, the choice of negative exponential distribution is acceptable. The expressions describing the distribution are respectively:

$$f(x) = \lambda e^{-\lambda x} \quad (1)$$

$$g(l) = \mu e^{-\mu l} \quad (2)$$

where  $x$  is the spacing variable ranging from 0 to  $+\infty$ ,  $\lambda$  is the reciprocal of the mean spacing,  $l$  is the trace length variable ranging also from 0 to  $+\infty$ ,  $\mu$  is the reciprocal of the mean trace length. In measurement, the statistical windows or scan-lines are finite and limited (the length of scan-line or the maximum distance of arbitrary two points in statistical window is referred to as  $L$ ). The data of spacing obtained can not be larger than  $L$ . The Eq. (1) is not suitable to describe the statistical regularity of the spacing data obtained from worksites or field outcrops. Frequently, the censored correction is performed for the Eq. (1). The result of censored correction is (Wu, 1995):

$$f_1(x) = \frac{\lambda}{1 - e^{-\lambda L}} e^{-\lambda x} \quad 0 < x \leq L \quad (3)$$

As stated above, the small discontinuities and micro-cracks are ignored in the measurement. Hence, the critical value of trace length between the small discontinuities and the large discontinuities is an important concept for measurement in worksites. Namely, the traces shorter than the critical value are considered as small discontinuities; and those longer than the critical value are considered as large discontinuities. Here, the critical value of trace length is defined as  $l_0$ . As we know, there are a large number of small discontinuities and micro-cracks in rock masses; and their spacing can not be very large. There must be a maximum value among these spacing of small discontinuities and micro-cracks. We can easily find out this maximum spacing value from the spacing data of small discontinuities obtained from worksites. This maximum value is defined as  $x_0$ . Obviously, the  $x_0$  is not an independent quantity, and has a close relation with the critical trace length value  $l_0$ . The  $x_0$  will definitely increase non-linearly as  $l_0$  increases.

Although the maximum value of spacing of small discontinuities is  $x_0$ , it does not mean that all the spacing values smaller than  $x_0$  only belong to small discontinuities and micro-cracks. Some of spacing values smaller than  $x_0$  would belong to large discontinuities. However, all the spacing values larger than  $x_0$  belong to large discontinuities. Now provided that the probabilistic density function of the spacing belonging to small discontinuities and large discontinuities is  $f_4(x)$  and  $f_5(x)$  in the range of 0 to  $x_0$ , following two expressions can be written

$$\int_0^{x_0} f_4(x)dx = 1 \quad \text{and} \quad \int_0^{x_0} f_5(x)dx = 1 \quad (4)$$

The total number of spacing of all discontinuities, including small discontinuities and large discontinuities is  $N$ . There are  $N + 1$  traces corresponding to the  $N$  spacings. It is reasonable to make the approximation:  $N \approx N + 1$ . According to the idea stated above, it is known that the spacing in the range of 0– $x_0$  consists of two parts, the first part is the spacing of small discontinuities; the second part is the spacing of large discontinuities. Then, the following expression can be obtained:

$$f_4(x)dx \cdot NI_0^l + f_5(x)dx \{NI_0^\infty - NI_{1x_0}^l\} = f_1(x)dx \cdot N \quad 0 < x \leq x_0 \quad (5)$$

where  $I$  and  $I_1$  is the definite integral of  $g(l)$  and  $f_1(x)$  over fixed intervals:

$$I_{l_1}^{l_2} = \int_{l_1}^{l_2} g(l)dl \quad \text{and} \quad I_{1x_1}^{x_2} = \int_{x_1}^{x_2} f_1(x)dx$$

Deleting the common factors  $N$  and  $dx$ , Eq. (5) can be simplified to:

$$f_4(x)I_0^l + f_5(x) \{I_0^\infty - I_{1x_0}^l\} = f_1(x) \quad 0 < x \leq x_0 \quad (6)$$

In the Eq. (5), the terms of  $NI_0^l$  and  $NI_0^\infty$  respectively stand for the total number of the small discontinuities and the large discontinuities. The term of  $NI_{1x_0}^l$  is the number of the large discontinuities with spacing value ranging from  $x_0$  to  $L$ ; it is a definite integral with the value of  $N(e^{\lambda x_0} - e^{\lambda L}) / (1 - e^{-\lambda L}) e^{\lambda(L+x_0)}$ . Correspondingly, the term of  $NI_0^\infty - NI_{1x_0}^l$  is the number of the large discontinuities with spacing value smaller than  $x_0$ .

So far as we know that the spacing of small discontinuities is generally small compared with the maximum value  $x_0$ ; however, their amount accounts for a large proportion in the all spacing of discontinuities. In the negative exponential distribution of spacing censored to  $L$ , the spacing of small discontinuities mainly concentrate at near the region of zero on the abscissa. As the value of spacing increases, the frequency of spacing of small discontinuities will fall sharply. Finally, the frequency of spacing of small discontinuities will preserve a very low level near the maximum value  $x_0$  (like that depicted in Fig. 1). According to this phenomenon and the distribution characteristics of the spacing of small discontinuities in fractured rock masses described above, the following hypothesis is made for derivation:

$$\frac{f_4(x)dx \cdot NI_0^l}{f_1(x)dx \cdot N} = A \left\{ \frac{1}{2} - \frac{1}{\pi} \arctan 50 \left( x - \frac{x_0}{2} \right) \right\} + B \quad 0 < x \leq x_0 \quad (7)$$

Removing the common factor  $N$  and  $dx$ , above expression become:

$$\frac{f_4(x)I_0^l}{f_1(x)} = A \left\{ \frac{1}{2} - \frac{1}{\pi} \arctan 50 \left( x - \frac{x_0}{2} \right) \right\} + B \quad 0 < x \leq x_0 \quad (8)$$

where  $f_4(x)dx \cdot NI_0^l$  is the amount of small discontinuities with spacing value  $x$  ( $0 < x \leq x_0$ ); and  $f_1(x)dx \cdot N$  is the total amount of

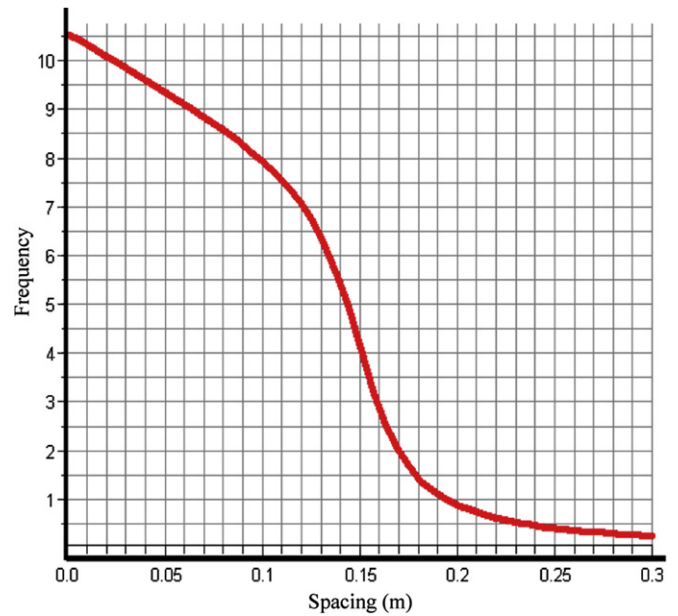


Fig. 1. The frequency of spacing belonging to small discontinuities near the region of 0 ( $x_0 = 0.3$ ).  $x_0$  is the maximum spacing measured from these small discontinuities.

discontinuities with spacing value also  $x$  ( $0 < x \leq x_0$ ), including the small discontinuities and large discontinuities. The above hypothesis is established based on the general shape of distribution curve of the spacing belonging to small discontinuities, and from the view of phenomenology. The ‘50’ is only an empirical coefficient here. A and B are the two correction coefficients. It is necessary to include these two correction coefficients, making the hypothesis flexible to describe the distribution curve of small spacing. Equation (8) shows the percentage of the spacing of small discontinuities whose value is  $x$  ( $0 < x \leq x_0$ ) (Fig. 9). The frequency of the spacing of small discontinuities near the region of zero is shown in Fig. 1 according to the hypothesis in Eq. (8).

Combining the Eqs. (2), (3), (6) and (8), linear equations are formed. Solving the equations, we can obtain following expressions:

$$f_4(x) = \frac{C\lambda e^{-\lambda x}}{(1 - e^{-\lambda L})(1 - e^{-\mu_0 L})} \quad (9)$$

$$f_5(x) = \frac{(1 - C)\lambda e^{-\lambda x}}{e^{-\mu_0 L} - e^{-\lambda x_0} + e^{-\lambda L} - e^{-(\mu_0 + \lambda)L}} \quad (10)$$

where

$$C = \left\{ A \left\{ \frac{1}{2} - \frac{1}{\pi} \arctan 50 \left( x - \frac{x_0}{2} \right) \right\} + B \right\} \quad (11)$$

According to Eq. (4), we get:

$$\int_0^{x_0} f_4(x)dx = \int_0^{x_0} \frac{C\lambda e^{-\lambda x}}{(1 - e^{-\lambda L})(1 - e^{-\mu_0 L})} dx = 1$$

$$\int_0^{x_0} A \left\{ \frac{1}{2} - \frac{1}{\pi} \arctan 50 \left( x - \frac{x_0}{2} \right) \right\} \lambda e^{-\lambda x} dx + \int_0^{x_0} B \lambda e^{-\lambda x} dx = (1 - e^{-\lambda L})(1 - e^{-\mu_0 L}) \quad (12)$$

Through some algebraic manipulations, we obtain an equation of A and B:

$$\left(B + \frac{1}{2}A\right)\left(1 - e^{-\lambda x_0}\right) + \frac{A}{\pi} \cdot D = \left(1 - e^{-\lambda L}\right)\left(1 - e^{-\mu l_0}\right) \quad (13)$$

Where  $D = -\int_0^{x_0} \arctan 50(x - x_0/2)\lambda e^{-\lambda x} dx$  is a definite integral which can be calculated using numerical method.

Next, we will establish the corrected probabilistic density function  $f_2(x)$  which is suitable to describe the statistical distribution of those spacing data with the statistical error obtained from worksites or outcrops. As stated above, the small discontinuities whose length is smaller than  $l_0$  generally are ignored in measuring. The probabilistic density function  $f_2(x)$  will not contain the spacing of small discontinuities. According to the probability theory, the  $f_2(x)$  can be defined as:

$$f_2(x)dx = \begin{cases} \frac{Nf_1(x)dx - NI_0^{l_0}f_4(x)dx}{NI_0^{l_0}} & 0 < x \leq x_0 \\ \frac{Nf_1(x)dx}{NI_0^\infty} & x_0 \leq x \leq L \end{cases} \quad (14)$$

Considering the Eqs. (2) and (8), and simplifying Eq. (14), we obtain:

$$f_2(x) = \begin{cases} \frac{f_1(x) - I_0^{l_0}f_4(x)}{I_0^\infty} = \frac{f_1(x)(1 - C)}{e^{-\mu l_0}} & 0 < x \leq x_0 \\ \frac{f_1(x)}{I_0^\infty} = \frac{f_1(x)}{e^{-\mu l_0}} & x_0 \leq x \leq L \end{cases} \quad (15)$$

---


$$E(x) = \int_0^L xf_2(x)dx = \int_0^{x_0} \frac{(1 - C)\lambda xe^{-\lambda x}}{(1 - e^{-\lambda L})e^{-\mu l_0}} dx + \int_{x_0}^L \frac{\lambda xe^{-\lambda x}}{(1 - e^{-\lambda L})e^{-\mu l_0}} dx$$

$$= \frac{\left\{ \left(\frac{A}{2} + B\right) \left(x_0 e^{-\lambda x_0} + \frac{e^{-\lambda x_0} - 1}{\lambda}\right) - L e^{-\lambda L} - \frac{e^{-\lambda L} - 1}{\lambda} + \frac{A\lambda}{\pi} \int_0^{x_0} \arctan 50\left(x - \frac{x_0}{2}\right) x e^{-\lambda x} dx \right\}}{(1 - e^{-\lambda L})\lambda e^{-\mu l_0}} = \bar{x} \quad (21)$$


---

Substituting Eqs. (2), (3) and (9) into Eq. (15):

$$f_2(x) = \begin{cases} \frac{(1 - C)\lambda e^{-\lambda x}}{(1 - e^{-\lambda L})e^{-\mu l_0}} & 0 < x \leq x_0 \\ \frac{\lambda e^{-\lambda x}}{(1 - e^{-\lambda L})e^{-\mu l_0}} & x_0 \leq x \leq L \end{cases} \quad (16)$$

$f_2(x)$  should be a continuous function in the range 0 to L. Accordingly,  $f_2(x)$  must be left continuous, right continuous and must have the same value at the point of  $x_0$ :

$$\frac{f_1(x_0)(1 - C)}{e^{-\mu l_0}} = \frac{f_1(x_0)}{e^{-\mu l_0}} \Rightarrow C|_{x=x_0} = 0 \quad (17)$$

And

$$C|_{x=x_0} = A\left\{\frac{1}{2} - \frac{1}{\pi} \arctan 25x_0\right\} + B = 0 \quad (18)$$

The above expression is actually another equation of A and B. Combining the Eqs. (13) and (18), we can obtain the solutions of A and B:

$$A = \frac{\pi(1 - e^{-\lambda L})(1 - e^{-\mu l_0})}{D + (1 - e^{-\lambda x_0})\arctan 25x_0} \quad (19)$$

$$B = \frac{\pi(1 - e^{-\lambda L})(1 - e^{-\mu l_0})\left(\frac{1}{\pi} \arctan 25x_0 - \frac{1}{2}\right)}{D + (1 - e^{-\lambda x_0})\arctan 25x_0} \quad (20)$$

As we can see from the Eqs. (19) and (20), the correction coefficients A and B both depend on the parameters  $\lambda$ ,  $\mu$ ,  $x_0$ ,  $l_0$  and L.

### 3. Estimation of the true distribution parameter of spacing

#### 3.1. Estimation of the parameter $\lambda$ based on the corrected model $f_2(x)$

The probabilistic density function  $f_2(x)$  reflects the statistical regularity of the spacing data with statistic errors obtained from worksites or outcrops. It can not describe the real distribution of spacing of all discontinuities in the fractured rock masses. The method of obtaining the true distribution parameter  $\lambda$  is presented as follow.

According to Eq. (16) and the probabilistic theory, the expected value (weighted mean spacing) of spacing under the distribution of  $f_2(x)$  is:

In Eq. (21),  $\lambda$  is the parameter we want to obtain which can relatively exactly describe the distribution of spacing of all discontinuities. The other parameters  $\mu$ ,  $x_0$ ,  $l_0$  and L all can be determined conveniently from the spacing data obtained from worksites or outcrops.  $\bar{x}$  is the mean value of the spacing measured on exposures, namely,  $\bar{x} = 1/n \sum_{i=1}^n x_i$ . Therefore, the problem of obtaining the parameter  $\lambda$  can be solved adopting Eq. (21). However, Eq. (21) is a highly nonlinear problem. Hence, it is very difficult and unrealistic to solve Eq. (21) analytically. In this study, we propose another method to determine  $\lambda$ . According to Eq. (21), a line graph can be plotted by taking  $\bar{x}$  as the longitudinal axis,  $\lambda$  as the abscissa (Fig. 2). From the line graph, we can easily determine the value of  $\lambda$  corresponding to the mean spacing  $\bar{x}$  on the line.

In application, we can calculate the mean spacing  $\bar{x}$  firstly from the measurement data obtained from worksites or outcrops. Then, the real distribution parameter  $\lambda$  of spacing of all discontinuities can be easily determined according to Fig. 2. It is also suggested to list a table to show the relationship between the  $\lambda$  and the mean spacing. Then, the linear or nonlinear interpolation method can be adopted to determine the values of  $\lambda$  based on the listed table. Here it is noted that the line graph or the table is significantly dependent on the four parameters of  $x_0$ ,  $\mu$ ,  $l_0$ , L. When applying the method proposed here to determine  $\lambda$ , we must plot the line graph or list

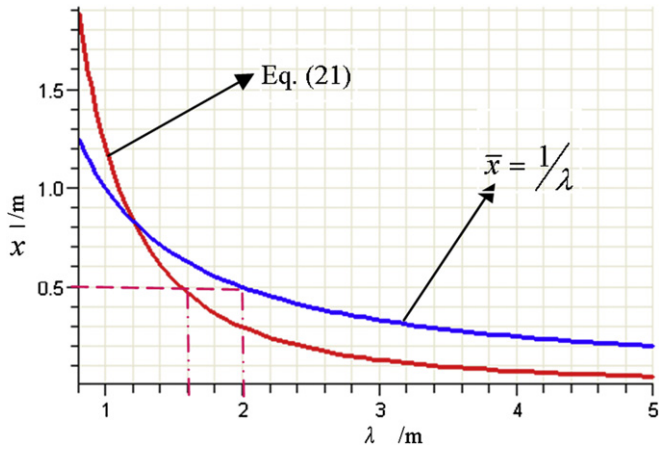


**Fig. 2.** Relation line graph between  $\bar{x}$  and  $\lambda$  according to Eq. (21).  $\bar{x} = 1/n \sum_{i=1}^n x_i$  is the mean value of the spacing measured on exposures.  $\lambda$  is the parameter describing the negative exponential distribution. In the complete negative exponential distribution,  $\lambda$  is the reciprocal of  $\bar{x}$ . This figure shows that the ignoring of small discontinuities in measurement has a significant effect on the distribution of measured spacing data. This graph is plotted assuming  $x_0 = 0.3$ ,  $\mu = 0.4$ ,  $l_0 = 0.5$ ,  $L = 100$ .

the table specially corresponding to the specific values of  $x_0$ ,  $\mu$ ,  $l_0$ ,  $L$ . Generally, the procedures of application of the method proposed in this study are shown in the Fig. 3.

In application, if we ignore all the discontinuities shorter than  $l_0$  in measuring, there will be no record of the trace length and the spacing of small discontinuities. It is very difficult for us to determine the maximum spacing value  $x_0$  of small discontinuities. To solve this problem, we should also record additionally some the spacing of these small discontinuities which are just little shorter than  $l_0$ . The maximum spacing value  $x_0$  of small discontinuities would be designated as 1.05 times the maximum value of the spacing of these small discontinuities.

### 3.2. Sensitivity analysis

The sensitivity analysis of  $\lambda$  is performed for  $\mu$ ,  $l_0$ ,  $x_0$  and  $L$ . The purpose is to check whether the true distribution parameter  $\lambda$  is sensitive to  $\mu$ ,  $l_0$ ,  $x_0$  and  $L$  according to the relationship of Eq. (21). When analyzing the sensitivity of  $\lambda$  to one of the four parameters, we set the other three parameters as a constant in calculation. Here we always designate the four parameter as  $x_0 = 0.3$ ,  $\mu = 0.4$ ,  $l_0 = 0.5$ ,  $L = 100$ ,  $\bar{x} = 0.4$  as in Fig. 2.

#### 3.2.1. The sensitivity to $\mu$ (reciprocal of mean trace length)

Fig. 4 shows the relationship curve between the true distribution parameter of spacing  $\lambda$  and the reciprocal of mean trace length  $\mu$ . It is easy to conclude that the real distribution parameter  $\lambda$  is moderately sensitive to the  $\mu$ . Therefore, it reminds us that we must carefully measure the trace length on exposures, and determine the mean trace length with the methods proposed in literature (Zhang and Einstein, 1998; Mauldon, 1998; Priest, 2004) which have eliminated the statistical error to some extent.

#### 3.2.2. The sensitivity to $l_0$ (the critical trace length)

Fig. 5 shows the relationship between the true distribution parameter of spacing  $\lambda$  and the critical trace length  $l_0$ . It also indicates that the  $\lambda$  is moderately sensitive to the critical trace length  $l_0$ . Therefore, we should carefully set an appropriate value of  $l_0$  in application of the correction model proposed in this study. Generally, under the precondition that the measuring work is not too time-consuming, the critical trace length  $l_0$  can be set as small as possible because the small value of  $l_0$  means a greater number of discontinuities can be measured.

#### 3.2.3. The sensitivity to $x_0$ (the maximum spacing value of small discontinuities)

Fig. 6 has shows the relationship between the true distribution parameter of spacing  $\lambda$  and the maximum spacing value of small

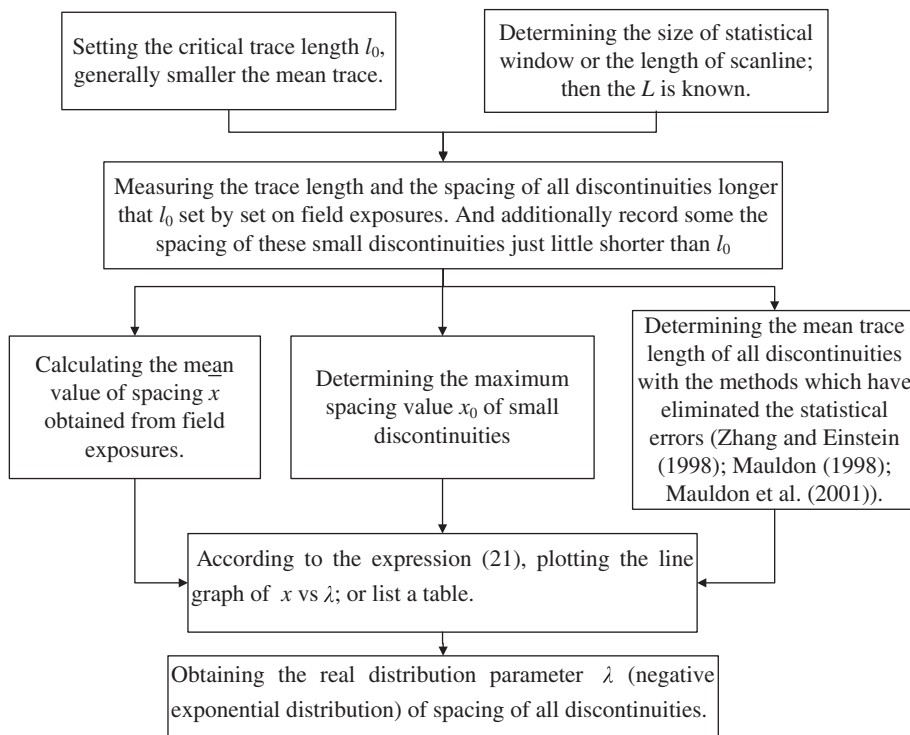


**Fig. 3.** Procedures of application of the correction theory presented in this study.

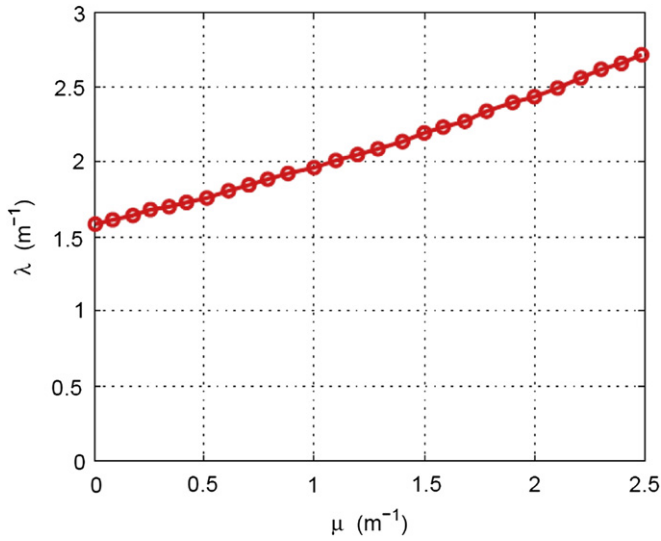


**Fig. 4.** Relationship between the real distribution parameter  $\lambda$  and the reciprocal of mean trace length of all discontinuities  $\mu$  ( $x_0 = 0.3, l_0 = 0.5, L = 100, \bar{x} = 0.4$ ).  $\lambda$  is the parameter describing the negative exponential distribution of the spacing of all discontinuities.

discontinuities  $x_0$ . From Fig. 6, it is can be seen that the real distribution parameter of spacing  $\lambda$  is not sensitive to the value of  $x_0$ . It is found that the  $\lambda$  varies in the range of 1.67–1.75 corresponding to the range of  $x_0$  from 0.05 to 1.5 m; and there are some oscillations for the value of  $\lambda$  when  $x_0$  is less than 0.8 m. Fortunately,  $\lambda$  is not sensitive to  $x_0$  as a whole. This is a very significant and valuable property. As stated above, it is relatively difficult to determine the accurate maximum spacing value of small discontinuities  $x_0$  in application. However, it only slightly affects the true distribution parameter  $\lambda$ . Therefore, it is acceptable to estimate the  $x_0$  with little error only because  $\lambda$  is not sensitive to  $x_0$  at all.

**3.2.4. The sensitivity to  $L$  (the length of scan-lines or the maximum distance of arbitrary two points in statistical windows)**

Fig. 7 illustrates the relationship between the true distribution parameter of spacing  $\lambda$  and  $L$ . It indicates clearly that the  $\lambda$  is very

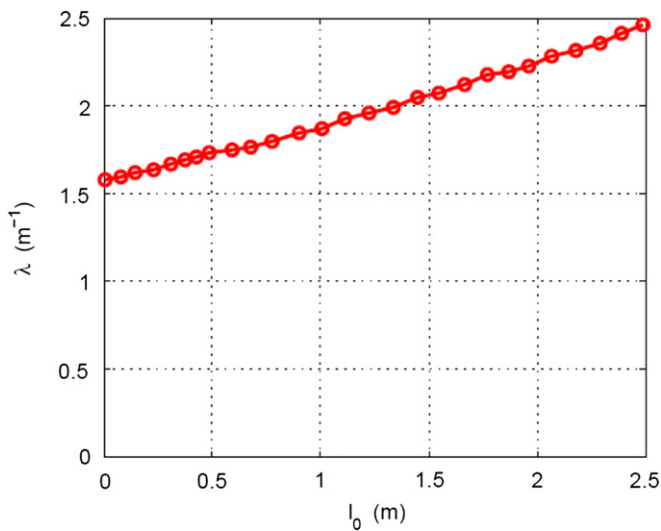


**Fig. 5.** Relationship between the real distribution parameter  $\lambda$  and the critical trace length  $l_0$  ( $x_0 = 0.3, \mu = 0.4, L = 100, \bar{x} = 0.4$ ).  $l_0$  is the critical trace length between the small discontinuities and large discontinuities.

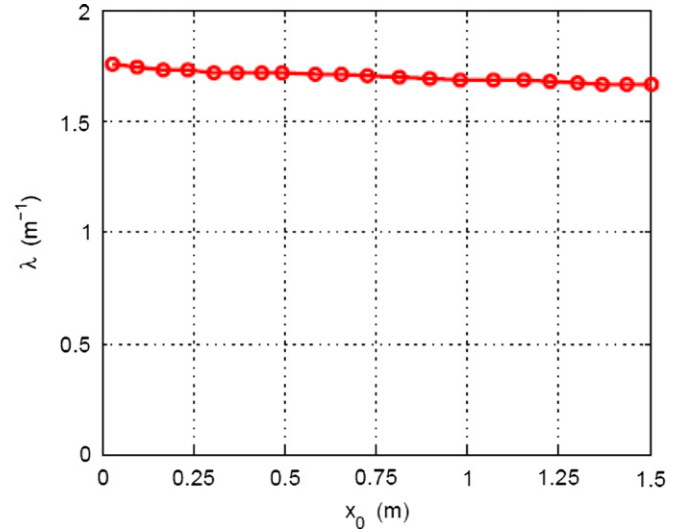


**Fig. 6.** Relationship between the real distribution parameter of spacing  $\lambda$  and the maximum spacing value of small discontinuities  $x_0$  ( $l_0 = 0.5, \mu = 0.4, L = 100, \bar{x} = 0.4$ ). It is shown that  $\lambda$  is not sensitive to  $x_0$ .

unstable when the value of  $L$  is less than 5 m; however it can quickly converge to its true value when the value of  $L$  is larger. Fig. 8 is drawn to study the convergence of  $\bar{x}$  when the  $L$  varies under the condition of  $\lambda = 1.73$  (which is the same with that in Fig. 2). It is indicated that  $\bar{x}$  is also unstable, and could not converge to the real value (0.4 m) when the value of  $L$  is less than 5 m. Once the value of  $L$  exceeds 5 m,  $\bar{x}$  will converge to its true value quickly. The two convergence characteristics remind us that the length of scan-lines or the maximum distance of arbitrary two points in statistical windows must be longer than 5 m in measurement on exposures.

**4. Verification of the correction model**

In fact, it is difficult to check the accuracy of the correction model because we can not obtain the spacing data of all small discontinuities in fractured rock masses. So we can not know about the probabilistic density function  $f_A(x)$  of the spacing of small

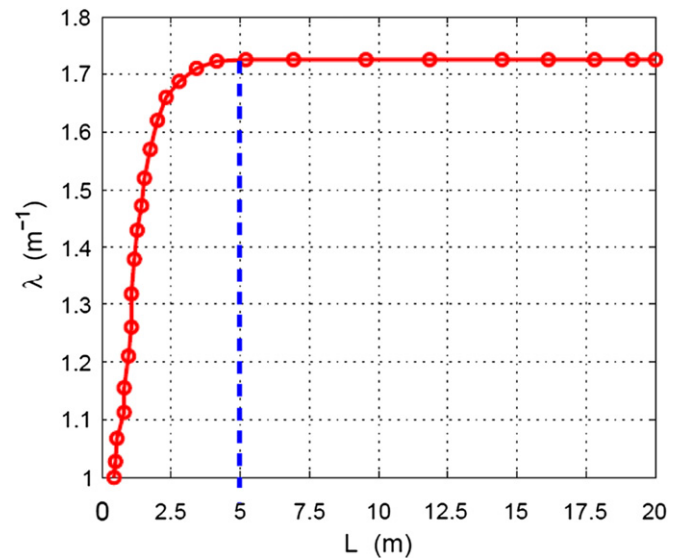


**Fig. 7.** Relationship between the real distribution parameter of spacing  $\lambda$  and  $L$ .  $L$  is the length of scan-line or the maximum distance of arbitrary two points in statistical window. It is indicated that the length of scan-line must be greater than 5 m.

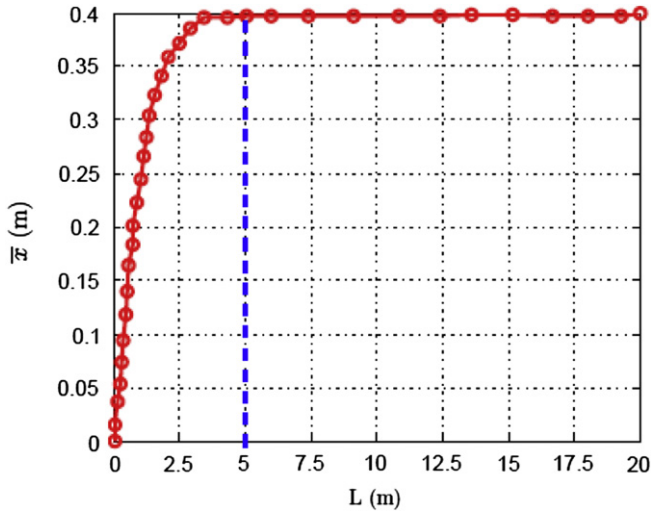


Fig. 8. Convergence analysis of  $\bar{x}$  when  $L$  varies under the condition that  $\lambda$  is set as 1.73 which is the same as that in Fig. 2.

discontinuities. Therefore, the best way to check the validity of the correction model  $f_2(x)$  is to examine whether  $f_2(x)$  could describe the statistical regularity of the spacing data of large discontinuities obtained at worksites or outcrops. In the following, two methods are adopted to check the validity of the corrected model  $f_2(x)$ .

#### 4.1. Simple verification with the ideal data

Supposed that we have a set of spacing data obtained from an outcrop using the method of statistical window or scan-line. The critical trace length is set as 0.5 m ( $l_0 = 0.5$ ). The length of scan-line or the maximum distance of arbitrary two points in the statistical window is 100 m ( $L = 100$ ). The mean trace length of all discontinuities is 2.5 m ( $\mu = 0.4$ ); the maximum value of spacing of small discontinuities is determined as 0.3 m ( $x_0 = 0.3$ ). The mean value of spacing measured from field exposures is 0.4 m. According to Fig. 2, the real distribution parameter  $\lambda$  is determined as 1.73.

According to Eqs. (9)–(11), (16), (19), (20), we obtain:

$$C = 0.4061 - 0.2823 \arctan(50x - 7.5)$$

$$f_4(x) = \frac{1.73Ce^{-1.73x}}{(1 - e^{-173})(1 - e^{-0.2})}$$

$$f_5(x) = \frac{1.73(1 - C)e^{-1.73x}}{e^{-0.2} - e^{-0.54} + e^{-173} - e^{-173.2}}$$

$$f_2(x) = \begin{cases} \frac{1.73(1 - C)e^{-1.73x}}{(1 - e^{-173})e^{-0.2}} & 0 < x \leq 0.3 \\ \frac{1.73e^{-1.73x}}{(1 - e^{-173})e^{-0.2}} & 0.3 \leq x \leq 100 \end{cases}$$

As the probabilistic density function, the  $f_4(x)$ ,  $f_5(x)$  and  $f_2(x)$  must satisfy that their integral value in the field of definition equal to 1. Through the method of numerical integration, the integral values of  $f_4(x)$ ,  $f_5(x)$  and  $f_2(x)$  in the field of definition are respectively:

$$\int_0^{x_0} f_4(x)dx = 0.9999999999 \text{ and } \int_0^{x_0} f_5(x)dx = 1.000000000$$

$$\begin{aligned} \int_0^{100} f_2(x)dx &= \int_0^{0.3} f_2(x)dx + \int_{0.3}^{100} f_2(x)dx \\ &= 0.2665530439 + 0.7334469561 \\ &= 1.0000000000 \end{aligned}$$

Their line graphs are shown in Figs. 9–12.

The line graph of the probabilistic density function  $f_2(x)$  is very similar to the lognormal distribution (Fig. 12). This is to say, the spacing data of large discontinuities with statistical error obtained from worksites or outcrops could approximately comply with the lognormal distribution according to the correction model  $f_2(x)$  proposed in this study. That proves to a great extent that the correction model  $f_2(x)$  is appropriate to describe the distribution regularity of spacing of large discontinuities.

#### 4.2. Verification with Monte Carlo simulation

##### 4.2.1. Single set of discontinuities

We consider the most simple distribution situation: only one set of discontinuities on the exposure which is 100 m long and 50 m wide. According to the previous results (Baghbanan and Jing, 2007; Mauldon, 1998; Min et al., 2004), generally, the distribution of center points of discontinuities approximately follows the Poisson process, namely a uniform random process in unit time or unit area. Here we also use this distribution characteristic for the center points of all discontinuities, and assume the density of center points of discontinuities (the amount of center points per unit area) is  $3 \text{ m}^{-2}$ . It means there are 15,000 center points and corresponding 15,000 discontinuities on the exposure with an area of  $5000 \text{ m}^2$ . Fig. 13 depicts the distribution of all center points generated using the Monte Carlo method according to the Poisson process. In this model, the trace length of discontinuities follows the negative exponential distribution. Here we assume the mean trace length of the 15,000 discontinuities is 0.9 m; accordingly, the trace length distribution parameter  $\mu = 1.11$ . These trace lengths are allocated to

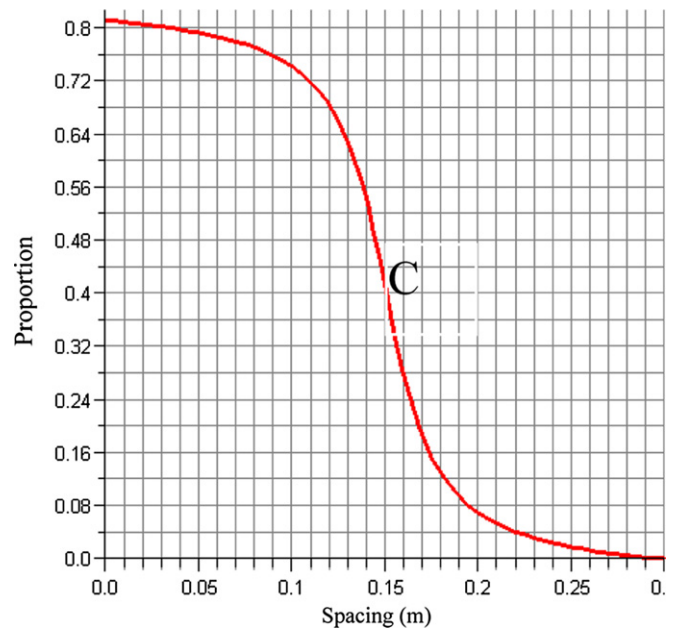


Fig. 9. The line graph of  $C$  corresponding to spacing ranging from 0 to  $x_0$  ( $x_0 = 0.3$ ). The function  $C$  actually represents the proportion between the amount of small discontinuities with spacing value  $x$  ( $0 < x \leq x_0$ ) and the total amount of discontinuities with spacing value  $x$  ( $0 < x \leq x_0$ ). This figure demonstrates that the spacing of small discontinuities is the dominant part in the region close to zero.

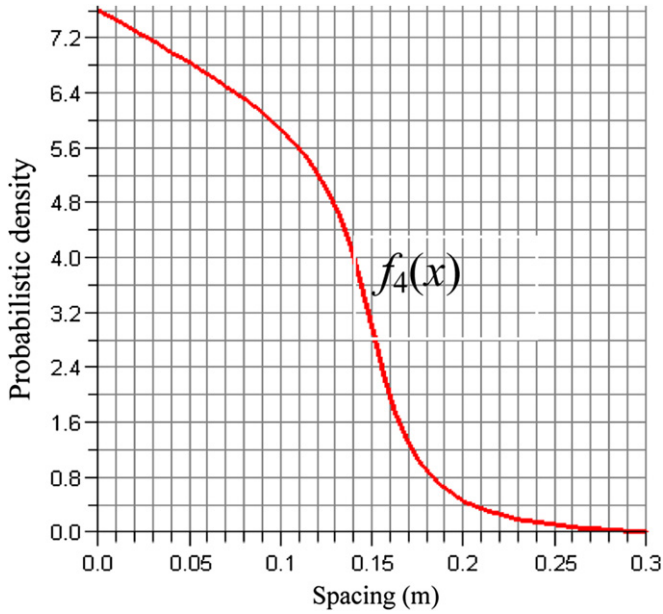


Fig. 10. Line graph of the probabilistic density function  $f_4(x)$ . It indicates that the frequency of the spacing of small discontinuities is mainly concentrates in the region close to zero; the frequency of the spacing of small discontinuities decreases sharply in the region around  $x_0/2$ , and maintains at a low level in the region near to  $x_0$  ( $x_0 = 0.3$ ).

the center points of discontinuities randomly. Then a simple discontinuity network model is formed after postulating all the discontinuities have the same angle of  $45^\circ$  with the horizontal direction.

In this study, only the scan-line method is adopted to measure the spacing here. The direction of scan-line, either horizontal or oblique, is expressed by  $y = kx + E$ , where  $k$  is the slope of scan-line,  $E$  is the intercept on the longitudinal axis. In measurement, only the spacing of those discontinuities longer than the critical trace length  $l_0$  and intersecting with the scan-line are measured. All

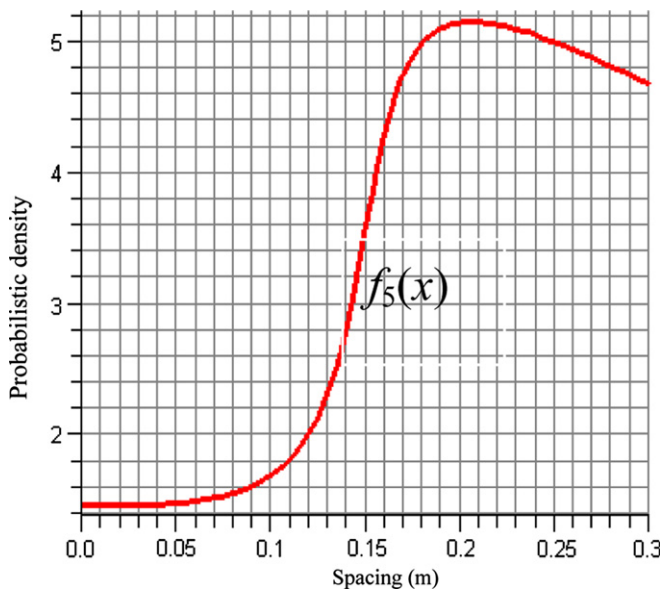


Fig. 11. Line graph of the probabilistic density function  $f_5(x)$ .  $f_5(x)$  is the distribution of the spacing of large discontinuities ranging from 0 to  $x_0$ . It is demonstrated that the frequency of the spacing of large discontinuities is apparently small in the region close to zero; while it is significantly large in the region close to  $x_0$ .

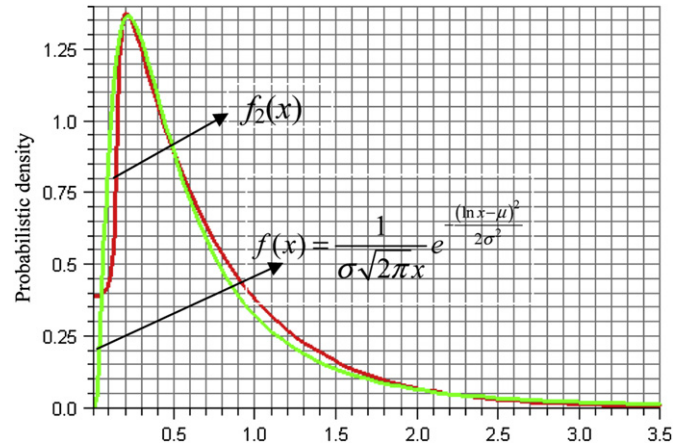


Fig. 12. Comparison between  $f_2(x)$  and ideal lognormal distribution ( $x_0 = 0.3$ ,  $\mu = 0.4$ ,  $l_0 = 0.5$ ,  $L = 100$ ,  $\lambda = 1.73$ ). The  $f_2(x)$  can be almost perfectly consistent with the lognormal distribution ( $\mu = -0.72$ ,  $\sigma = 0.9$ ) except the region close to zero.

measurement procedures follow the popular method suggested by ISRM (Brown, 1981) and the procedures stated in Fig. 3, and are implemented by the self-programmed code and the mathematical software Matlab and Maple.

First of all, the scan-line is horizontal. The intercept  $E$  is set as 45 m, 35 m, 25 m and 15 m respectively. According to the definition of the  $L$ , it is 100 m. In simulated measurement, the critical trace length  $l_0$  is assumed as 0.5 m and 0.8 m respectively for each intercept. Here, we obtain the value of  $x_0$  through measuring the spacings of discontinuities shorter than critical trace length  $l_0$  in a window corresponding to each scan-line (Fig. 13). For each intercept  $E$  and critical trace length  $l_0$ , a set of spacing of discontinuities longer than  $l_0$  is obtained through the developed source code. Then the mean spacing and the variance can be determined. Finally, the true distribution parameter  $\lambda$  of spacing of all discontinuities can be determined according to Eq. (21). The results of Monte Carlo simulation for this simple model are listed in Table 1.

For the cases of an oblique scan-line (@ in Fig. 13), taking similar procedures as for the horizontal scan-line, we also can obtain a series of data and the true distribution parameter  $\lambda$  which is listed in Table 2.

From the Table 1 and the Table 2, it is easy to find that the parameter  $\lambda$  is in the range of 1.91–2.45. Its mean value is 2.104, and the variance is 0.0255. From the variance, we know that the concentration degree of  $\lambda$  is high. Another property of the real distribution parameter  $\lambda$  found from the Table 1 and Table 2 is that  $\lambda$  will increase slightly when the critical trace length  $l_0$  increases from 0.5 m to 0.8 m.

We further measure the spacing of all discontinuities which intersect with each scan-line with different intercept  $E$ . The purpose is to check whether the values of  $\lambda$  listed in Table 1 and Table 2 can really describe the distribution regularity of spacing of all discontinuities on the exposure modeled. This kind of distribution of spacing of all discontinuities intersecting with scan-lines (without considering the critical trace length  $l_0$ ) is the true distribution of spacing in the model. It is referred to as the true complete distribution of the spacing.

All the spacing of discontinuities intersecting with the horizontal scan-lines  $y = E$  in the model are measured and recorded, where the intercept  $E$  are set as 45 m, 40 m, 35 m, 30 m, 25 m, 20 m, 15 m, 10 m respectively. There are eight sets of spacing data, and in total about 4000 spacings are obtained from the model. The histogram of the eight sets of spacings is shown in Fig. 14. Through statistical fitting, it

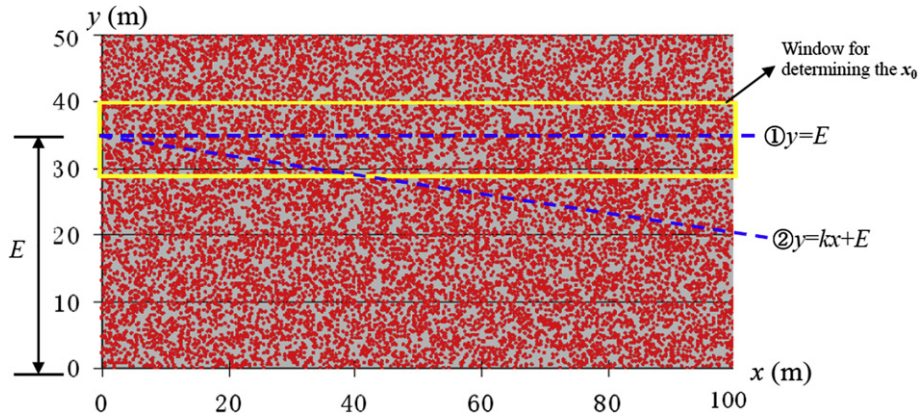


**Fig. 13.** Distribution of center points of all discontinuities in model. The center points of all discontinuities follow Poisson process. The density of center points is assumed as  $3 \text{ m}^{-2}$ . The solid window is used to determine the value of  $x_0$  through measuring the spacing of small discontinuities shorter than critical trace length  $l_0$ .

is found that the negative exponential distribution (the pdf is  $f(x) = \lambda e^{-\lambda x}$ ) can best describe it when the mean value and variance is 0.3715 m, 0.1426 respectively. Finally, according to the statistical theory, we know that the true complete distribution parameter of spacing  $\lambda_{\text{true}}$  is 2.692.

Comparing the values of predicted  $\lambda$  listed in Table 1 and Table 2 with  $\lambda_{\text{true}}$ , we find that the differences between the  $\lambda$  and  $\lambda_{\text{true}}$  are significant. The differences vary in the range of 17%–29%. Another point is that all the  $\lambda$  values obtained by the correction theory proposed in the previous sections are smaller than  $\lambda_{\text{true}}$ . The main reason for this phenomenon is that there is only one set of discontinuities. Additionally, some problems always exist in the model due to some unavoidable flaws when allocating the trace lengths to center points of discontinuities randomly. For example, the spacing of two large discontinuities (the trace lengths can be longer than 4 m) may be very small. In fact, that is not likely to exist in the real world. All these factors may make the small spacing account for a larger proportion in the model, and the mean spacing become smaller than that of a normal model which may exist in nature.

Many spacing data have been obtained for different intercepts  $E$  and different critical trace lengths  $l_0$ . Here, only the distribution histograms of the spacing obtained by the scan-lines  $k = 0, E = 35/25 \text{ m}, l_0 = 0.8 \text{ m}$  are shown and analyzed as examples for the sake of simplicity (Fig. 15).

From Fig. 15 (a), (b), it is not difficult to conclude that the corrected probabilistic density function  $f_2(x)$  proposed in this study is better than the lognormal distribution to describe the true distribution of spacing obtained from the model when the critical trace length  $l_0$  is considered. This proves to a great extent that the correction theory considering the statistical error presented in this study is acceptable.

**Table 1**  
Results of Monte Carlo simulation for the model only containing one set of discontinuities (the slope of scan-line  $k = 0$ ).

$E$ (m)	$L$ (m)	$l_0$ (m)	$x_0$ (m)	Mean spacing (m)	Variance of spacing	$\lambda$	Difference with $\lambda_{\text{true}}$ (%)
45	100	0.5	0.252	0.4447	0.0267	1.93	28.3
	100	0.8	0.230	0.505	0.0277	2.07	23.1
35	100	0.5	0.261	0.4017	0.0249	1.98	26.4
	100	0.8	0.312	0.4475	0.0265	2.22	17.5
25	100	0.5	0.242	0.3644	0.0276	2.12	21.2
	100	0.8	0.323	0.4110	0.0309	2.30	14.6
15	100	0.5	0.217	0.4110	0.355	2.01	25.3
	100	0.8	0.353	0.4745	0.0334	2.14	20.5

4.2.2. Multiple sets of discontinuities

There are frequently several sets of discontinuities on an exposure of field sites or outcrops, rather than only containing one set. In this section, a complex model is generated to verify the correction theory presented in previous sections, and to check whether the result determined according to Eq. (21) can describe the statistical regularity of the spacing of all discontinuities.

Four sets of discontinuities on an exposure (100 m long  $\times$  50 m wide) are considered. As in the above simple model, we continue to assume the density of center points of discontinuities is  $3 \text{ m}^{-2}$ , and the four sets of discontinuities have the same number of traces on the exposure. This means that there are 3750 traces for each set of discontinuities. The center points of all four sets of discontinuities follow the Poisson's process. The trace lengths of all four sets of discontinuities follow the negative exponential distribution, the mean trace lengths are 1.5 m, 2.0 m, 2.5 m, and 3.0 m respectively. The angles between the four sets of discontinuities and the horizontal axis are  $30^\circ, 45^\circ, 90^\circ, 135^\circ$  respectively. The distribution of the four sets of discontinuities on the exposure modeled is sketched in Fig. 16.

In this complex model, there are four sets of discontinuities with different mean trace length. Therefore, the distribution parameter of trace length  $\mu$  for this complex model needs to be determined by the complete trace length distribution of the four sets of discontinuities. Through a simple statistical analysis, the mean trace length of this complex model is determined as 2.25 m, then the parameter  $\mu$  is 0.444. Here, for the sake of simplicity, only the horizontal scan-lines are adopted to measure the spacing of discontinuities. Four intercepts  $E$  (45 m, 35 m, 25 m, and 15 m respectively) and three critical trace lengths  $l_0$  (1.5 m, 1.8 m and 2.0 m) for each intercept are designated in measuring. Finally, taking a similar method and procedures used for the single set of discontinuities model, a series of spacing data and results are obtained which are listed in the Table 3

**Table 2**  
Results of Monte Carlo simulation for the model just containing one set of discontinuities (the slope of scan-line  $k = \tan(150^\circ) = -\sqrt{3}/3$ ).

$E$ (m)	$L$ (m)	$l_0$ (m)	$x_0$ (m)	Mean spacing (m)	Variance of spacing	$\lambda$	Difference with $\lambda_{\text{true}}$ (%)
45	78	0.5	0.247	0.3101	0.0257	2.29	18.4
	78	0.8	0.360	0.3553	0.0306	2.45	8.99
35	60.6	0.5	0.255	0.4503	0.0262	1.91	29.0
	60.6	0.8	0.337	0.5237	0.0305	2.04	24.2
25	43.3	0.5	0.239	0.5276	0.0280	1.95	27.6
	43.3	0.8	0.315	0.5992	0.0341	2.05	23.8

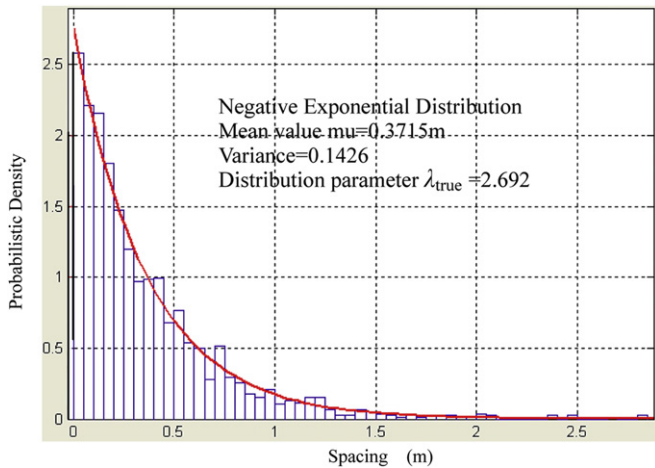


Fig. 14. Histogram of the spacing of all discontinuities intersecting with the eight scan-lines. Both the large discontinuities and small discontinuities are included, without considering the critical trace length  $l_0$ .

From the Table 3, we know that the predicted true distribution parameter  $\lambda$  is in the range of 1.62–1.69. The mean value of  $\lambda$  is 1.6475, and the variance is  $8.3864 \times 10^{-4}$ . The small variance indicates that there is a very high concentration degree for  $\lambda$ .

All the spacing of discontinuities intersecting with the horizontal scan-lines  $y = E$  ( $E = 45$  m, 35 m, 25 m, 15 m respectively) are measured for determining the true complete distribution

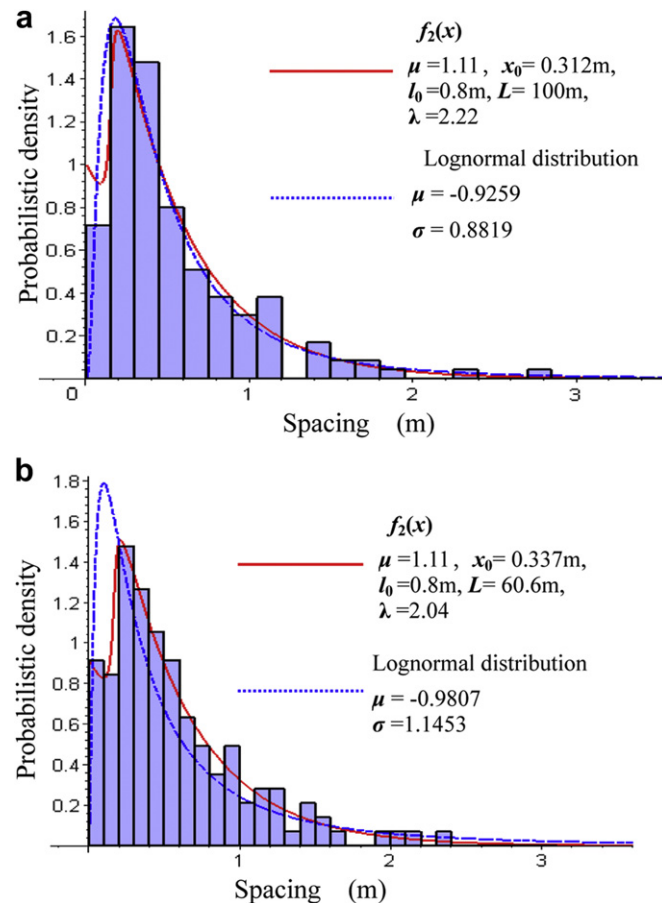


Fig. 15. Distribution histograms of the spacing measured by the four scan-lines: (a)  $k = 0$ ,  $E = 35$  m,  $l_0 = 0.8$  m, (b)  $k = -\sqrt{3}/3$ ,  $E = 35$  m,  $l_0 = 0.8$  m.

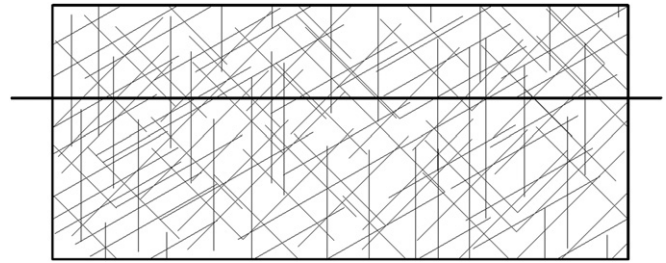


Fig. 16. Sketched distribution of the four sets of discontinuities on the exposures modeled.

parameter of spacing  $\lambda_{true}$  of this complex model. Four sets of spacing data, in a total of about 2000 spacings, are obtained from this complex model. The histogram of the four sets of spacing is shown in Fig. 17. Through the statistical fitting, it is also found that the negative exponential distribution can best describe the statistical regularity when the mean value and variance are 0.5821 m, 0.3427 respectively. Finally, according to the statistical theory, the true complete distribution parameter of spacing  $\lambda_{true}$  of this complex model is determined as 1.718.

The differences between the  $\lambda_{true}$  of this complex model and the  $\lambda$  predicted by the correction theory presented in this study are in the range of 1.63%–7.45% (Table 3). The mean difference is only 4.1%. This again proves that the correction theory and the corrected probabilistic density function  $f_2(x)$  are reasonable and acceptable.

Here, for simplicity, we only illustrate the spacing obtained by the scan-lines (a)  $k = 0$ ,  $E = 45$  m,  $l_0 = 1.8$  m and (c)  $k = 0$ ,  $E = 25$  m,  $l_0 = 1.8$  m. Their distribution histograms are shown in Fig. 18. From Fig. 18 (a), (b), it is concluded that the corrected probabilistic density function  $f_2(x)$  proposed in this study can well describe the statistical regularity of the spacing of large discontinuities longer than the critical trace length  $l_0$ .

### 5. Discussion

Discontinuities exist in rock masses with various shapes in 3D space. Generally, the circle and ellipse are the popular shapes used in research to approximately study the mechanical and hydraulic properties of the fractured rock masses. Whatever the shapes of discontinuities are, if the discontinuities intersect with the outcrop exposures, then the discontinuities will be seen as straight lines on exposures. Actually, the vertical distances between these lines are not the true spacing, but the apparent spacing. Therefore, when measurement is carried out on field sites, some modification should be made for these apparent spacing to obtain the real spacing.

Table 3

Results of Monte Carlo simulation for complex model containing four sets of discontinuities (the slope of scan-line  $k = 0$ ). There are four intercepts, and three critical trace lengths for each intercept are designated ( $\mu = 0.444$ ).

$E$ (m)	$L$ (m)	$l_0$ (m)	$x_0$ (m)	Mean spacing (m)	Variance of spacing	$\lambda$	Difference with $\lambda_{true}$ (%)
45	100	1.5	0.6731	0.6479	0.2966	1.63	5.10
	100	1.8	0.7243	0.6748	0.2097	1.67	2.79
	100	2.0	0.8030	0.6957	0.1974	1.69	1.63
35	100	1.5	0.6457	0.6859	0.2048	1.59	7.45
	100	1.8	0.6978	0.7075	0.2344	1.64	4.54
	100	2.0	0.8423	0.7342	0.2976	1.64	4.54
25	100	1.5	0.6745	0.6537	0.3452	1.62	5.70
	100	1.8	0.7460	0.6908	0.3578	1.65	3.96
	100	2.0	0.8021	0.7215	0.2876	1.66	3.38
15	100	1.5	0.6635	0.6465	0.1198	1.63	5.10
	100	1.8	0.7340	0.6811	0.2589	1.66	3.38
	100	2.0	0.7843	0.7058	0.3004	1.69	1.63

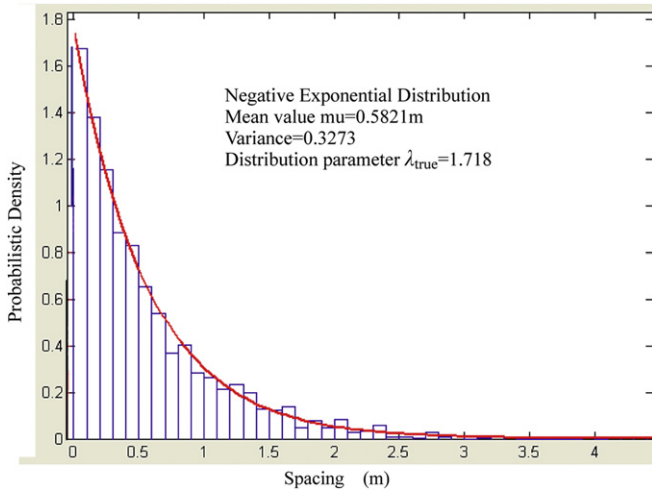


**Fig. 17.** Histogram of the spacing of all discontinuities intersecting with the four scan-lines in the complex model. The critical trace length  $l_0$  is not considered.

If the dip angle of discontinuities is  $\alpha$  ( $0 \leq \alpha \leq 90^\circ$ ), the angle between discontinuities plane and the exposure is  $\beta$  ( $0 \leq \beta \leq 90^\circ$ ), and distance of scan-line between two discontinuity lines on exposure is expressed as  $l$ , then the relationship between the apparent spacing and the true spacing is expressed as:

$$sp_{\text{true}} = l \sin \alpha \sin \beta \quad (22)$$

where  $sp_{\text{true}}$  is the true spacing of discontinuities.

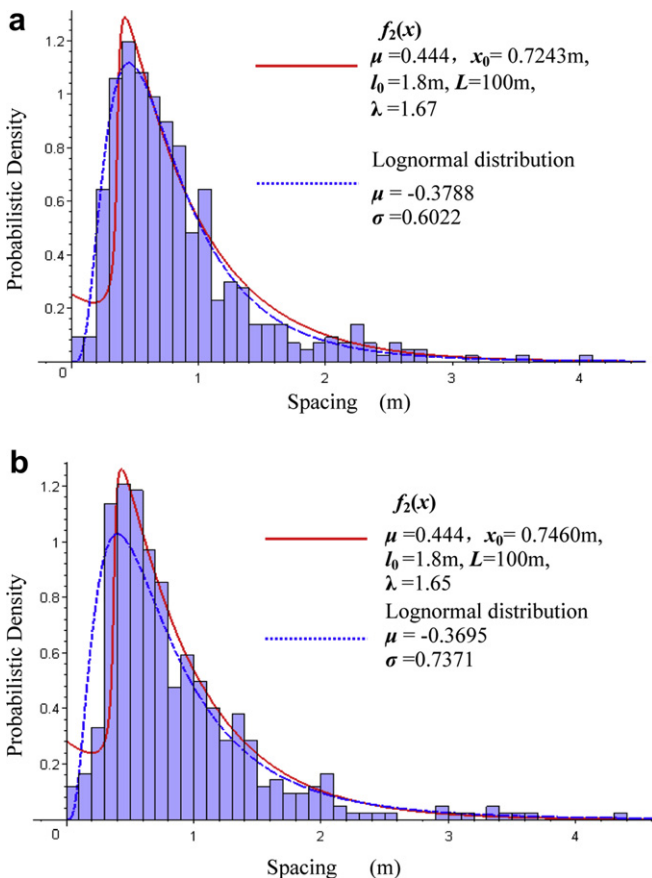


**Fig. 18.** Distribution histograms of the spacing measured by the four scan-lines: (a)  $k = 0, E = 45 \text{ m}, l_0 = 1.8 \text{ m}$ , (b)  $k = 0, E = 25 \text{ m}, l_0 = 1.8 \text{ m}$ .

On a natural exposure, there are usually several sets of discontinuities. The discontinuities belonging to the same set are parallel or approximately parallel with each other. The spacing should be measured set by set.

A great number of previous research results indicate that the trace length of all discontinuities on an exposure essentially follows the negative exponential distribution. However, because some small discontinuities and all micro discontinuities are ignored in measurement, the trace length of discontinuities generally do not follow the negative exponential distribution, but may be follow the lognormal distribution or other similar distributions. Therefore, the mean value of the trace lengths collected from exposures is not the real mean trace length. Fortunately, some methods to determine the real mean trace length have been proposed in some previous literature (Zhang and Einstein, 1998; Mauldon, 1998; Mauldon et al., 2001). From the analysis in previous section, we know that the mean trace length is a significant parameter in the correction theory proposed in this study; and the true distribution parameter  $\lambda$  is sensitive to it. Therefore, it is very important to determine the mean trace length exactly in the application of the correction theory in practical engineering.

The maximum spacing  $x_0$  of small discontinuities shorter than critical trace length  $l_0$  is relatively difficult to determine exactly in practice due to the fact that we almost ignore all those small discontinuities. Fortunately, the real distribution parameter  $\lambda$  is very insensitive to  $x_0$ . Therefore, small errors in  $x_0$  will not create much error in  $\lambda$ . In application, in order to determine a reasonable value of  $x_0$ , we must also additionally measure some spacing of small discontinuities shorter than the  $l_0$  on an exposure. The value of  $x_0$  could be designated as 1.05 times of the maximum spacing among these measured spacing of small discontinuities.

In this study, the correction theory is only verified adopting the 2D models generated by Monte Carlo simulation. In fact, the correction theory is applicable for 3D model which is most close to practical rock engineering. Verification of the correction theory proposed in this study by using the 3D Monte Carlo model is an interesting topic that needs to be further studied in future.

As the basis of the correction theory proposed in this study, an assumption that the distribution of the spacings of small discontinuities whose value is  $x$  ( $0 < x \leq x_0$ ) could be described by Eq. (7) is made. Although the hypothesis is established based on the engineering experience, and from the view of phenomenology, Eq. (7) can well reflect the spacing distribution regularity of small discontinuities. An important evidence is that the distribution shape of the 712 spacing data of small discontinuities obtained from a cut surface (320 mm  $\times$  70 mm) of a rock block obtained by Gomez and Laubach (2006) using the petrographic microscope is basically consistent with Eq. (7). Hence, the rationality of the assumption seems to be acceptable. Furthermore, from the results of Monte Carlo simulation, the corrected probabilistic density function  $f_2(x)$  can always well describe the statistical regularity of spacing obtained from the simple or complex model when the critical trace length  $l_0$  is considered. That suggests again that the assumption is acceptable.

## 6. Conclusion

The mechanical and hydraulic properties of fractured rock masses are generally controlled by the distribution characteristics of discontinuities developed randomly in rock masses. Field measurement is the only way to obtain the distribution characteristics of discontinuities in practical engineering. However, in the field measurement at outcrops, the data of spacing and length obtained from outcrops do not comply with the negative exponential distribution because of some statistical errors or sampling

errors. In this study, a new correction model is proposed to describe the distribution regularity of the spacing data with statistical errors obtained from outcrops. Based on the correction model, a new method is presented to determine the true distribution parameter of spacing of all discontinuities (negative exponential distribution).

The analysis results indicate that the real distribution parameter  $\lambda$  is moderately sensitive to the parameter  $\mu$  (reciprocal of mean trace length) and the critical trace length  $l_0$ ; and completely insensitive to the maximum spacing of small discontinuities  $\chi_0$ . These kinds of sensitivity characteristics of  $\lambda$  require that the mean trace length must be exactly determined and the critical trace length  $l_0$  must be designated as a reasonable value according to the real situation on outcrops. Another conclusion from the sensitivity analysis is that the length of scan-line should be longer than 5 m; otherwise,  $\lambda$  can not converge to its true value from the view of pure theory. The verification is performed for the correction theory and the corrected probabilistic density function  $f_2(x)$  by adopting a simple 2D model only containing a set of discontinuities and a complex 2D model containing four sets of discontinuities generated by the Monte Carlo Method. The simulation results of the two models indicate that the correction theory is reasonable and reliable, and the corrected probabilistic density function  $f_2(x)$  can well describe the statistical regularity of the spacing of discontinuities when the critical trace length  $l_0$  is considered.

## Acknowledgments

This research was supported by National Natural Science Foundation of China (NNSFC), project No. 41030749.

## References

- Baecher, G.B., 1983. Statistical analysis of rock mass fracturing. *Journal of Mathematical Geology* 15, 329–347.
- Baghbanan, A., Jing, L., 2007. Hydraulic properties of fractured rock masses with correlated fracture length and aperture. *International Journal of Rock Mechanics and Mining Sciences* 44, 704–719.
- Brown, E.T., 1981. ISRM Suggested Methods: Rock Characterization, Testing and Monitoring. Pergamon, London.
- Castaing, C., Genter, A., Chiles, J.P., Bourguin, B., Ouillon, G., 1997. Scale effects in nature fracture networks. *International Journal of Rock Mechanics and Mining Sciences* 34, 45.e1–45.e18.
- Deng, R.G., Zhang, Z.Y., Huang, R.Q., 1996. The structural plane characteristics of rock mass in No.1 Jinping hydropower station. *Journal of Geological Hazards and Environment Preservation* 7, 35–40.
- Einstein, H.H., Beacher, B.G., 1983. Probabilistic and statistical methods in engineering Geology specific methods and examples part I: exploration. *Rock Mechanics and Rock Engineering* 16, 39–72.
- Gillespie, P.A., Howard, C.B., Walsh, J.J., Watterson, J., 1993. Measurement and characterisation of spatial distributions of fractures. *Tectonophysics* 226, 113–141.
- Gomez, L.A., Laubach, S.E., 2006. Rapid digital quantification of microfracture populations. *Journal of Structural Geology* 28, 408–420.
- Kulatilake, P.H.S.W., Chen, J., Teng, J., Shufang, X., Pan, G., 1996. Discontinuity geometry characterization in a tunnel close to the proposed permanent ship-lock area of the three gorges dam site in China. *International Journal of Rock Mechanics and Mining Science and Geomechanics Abstracts* 33, 255–277.
- Kulatilake, P.H.S.W., Wathugala, D.N., Stephansson, O., 1993. Joint network modeling with a validation exercise in Strip mine, Sweden. *International Journal of Rock Mechanics and Mining Sciences and Geomechanics Abstracts* 30, 503–526.
- Kulatilake, P.H.S.W., He, W., Um, J., Wang, H., 1997. A physical model study of jointed rock mass strength under uniaxial compressive loading. *International Journal of Rock Mechanics and Mining Sciences* 34, 165.e1–165.e15.
- Kulatilake, P.H.S.W., Um, J., Wang, M., Escandon, R.F., Varvaiz, J., 2003. Stochastic fracture geometry modeling in 3-D including validations for a part of Arrowhead East Tunnel, California, USA. *Engineering Geology* 70, 131–155.
- Larsen, B., Grunnaleite, I., Gudmundsson, A., 2009. How fracture systems affect permeability development in shallow-water carbonate rocks: an example from the Gargano Peninsula, Italy. *Journal of Structural Geology* 32, 1212–1230.
- Lin, C.T., Amadei, B., Jung, J., Dwyer, J., 1996. Extensions of discontinuous deformation analysis for jointed rock masses. *International Journal of Rock Mechanics and Mining Science and Geomechanics Abstracts* 33, 671–694.
- Liu, D.A., Wang, S.J., Li, L.Y., 2000. Investigation of fracture behaviour during rock mass failure. *International Journal of Rock Mechanics and Mining Sciences* 37, 489–497.
- Lemy, F., Hadjigeorgiou, J., 2003. Discontinuity trace map construction using photographs of rock exposures. *International Journal of Rock Mechanics and Mining Sciences* 40, 903–917.
- Mauldon, M., Dunne, W.M., Rohrbach Jr., M.B., 2001. Circular scanlines and circular windows: new tools for characterizing the geometry of fracture traces. *Journal of Structural Geology* 23, 247–258.
- Mauldon, M., 1998. Estimating mean fracture trace length and density from Observations in Convex windows. *Rock Mechanics and Rock Engineering* 31, 201–216.
- Min, K.B., Jing, L., Stephansson, O., 2004. Determining the equivalent permeability tensor for fractured rock masses using a stochastic REV approach: method and application to the field data from Sellafeld, UK. *Hydrogeology Journal* 12, 497–510.
- Narr, W., Suppe, J., 1991. Joint spacing in sedimentary rocks. *Journal of Structural Geology* 13, 1037–1048.
- Odonne, F., Lézin, C., Massonnat, G., Escadeillas, G., 2007. The relationship between joint aperture, spacing distribution, vertical dimension and carbonate stratification: an example from the Kimmeridgian limestones of Pointe-du-Chay (France). *Journal of Structure Geology* 29, 746–758.
- Park, H.J., West, T.R., 2001. Development of a probabilistic approach for rock wedge failure. *Engineering Geology* 59, 233–251.
- Pascal, C., Angelier, J., 1997. Distribution of joints: probabilistic modeling and case study near Cardiff (Wales, UK). *Journal of Structure Geology* 19, 1273–1284.
- Priest, S.D., Hudson, J.A., 1976. Discontinuity spacing in rock. *International Journal of Rock Mechanics and Mining Sciences and Geomechanics Abstract* 13, 135–148.
- Priest, S.D., Hudson, J.A., 1981. Estimation of discontinuity spacing and trace length using scanline survey. *International Journal of Rock Mechanics and Mining Sciences and Geomechanics Abstract* 18, 183–197.
- Priest, S.D., 2004. Determination of discontinuity size distributions from scanline data. *Rock Mechanics and Rock Engineering* 37, 347–368.
- Ruf, J.C., Rust, K.A., Engelder, T., 1998. Investigating the effect of mechanical discontinuities on joint spacing. *Tectonophysics*, 245–257.
- Sari, M., 2009. The stochastic assessment of strength and deformability characteristics for a pyroclastic rock mass. *International Journal of Rock Mechanics & Mining Sciences* 46, 613–626.
- Simpson, G.D.H., 2000. Symmetamorphic vein spacing distributions: characterisation and origin of a distribution of veins from NW Sardinia, Italy. *Journal of Structure Geology* 22, 335–348.
- Tai, T.W., Huang, T.H., 2009. A constitutive model for the deformation of a rock mass containing sets of ubiquitous joints. *International Journal of Rock Mechanics and Mining Sciences* 46, 521–530.
- Toth, T.M., 2009. Determination of Geometric parameters of fracture networks using 1D data. *Journal of Structural Geology* 32, 878–885.
- Wallis, P.F., King, M.S., 1980. Discontinuity spacings in a crystalline rock. *International Journal of Rock Mechanics and Mining Sciences and Geomechanics Abstract* 17, 63–67.
- Warburton, P.M., 1980. A stereological interpretation of joint trace data. *International Journal of Rock Mechanics and Mining Sciences and Geomechanics* 17, 181–190.
- Wu, F.Q., 1995. *The Principal of Statistical Rock Mechanics*. China University of Geosciences Press, Wuhan.
- Zhang, L., Einstein, H.H., 1998. Estimating the mean trace length of rock discontinuities. *Rock Mechanics and Rock Engineering* 31, 217–235.
- Zhang, M.J., Liu, H.B., Zhu, Y.J., 2007. Determination of trace Auum in Tungsten Samples by Flame Atomic Absorption Spectrometry after Cloud point Extraction. *China Tungsten Industry* 22, 36–38.
- Zhou, N.Q., Zhu, X.Y., Li, Q.G., Shang, Y.J., 2000. Simulation of joint cracks in reaction zone of Qinshan nuclear power station in its third engineering stage. *Journal of Engineering Geology* 8, 466–470.